

Application of the Suzuki-Miyaura Reaction for the Postfunctionalization of the Benzo[4,5]thiazolo[3,2-c][1,3,5,2]oxadiazaborinine Core: An Approach towards Fluorescent Dyes

Mykhaylo A. Potopnyk, Dmytro Volyniuk, Roman Luboradzki, Magdalena Ceborska, Iryna Hladka, Yan Danyliv, and Juozas Vidas Grazulevicius

J. Org. Chem., **Just Accepted Manuscript** • DOI: 10.1021/acs.joc.9b00566 • Publication Date (Web): 16 Apr 2019

Downloaded from <http://pubs.acs.org> on April 18, 2019

Just Accepted

"Just Accepted" manuscripts have been peer-reviewed and accepted for publication. They are posted online prior to technical editing, formatting for publication and author proofing. The American Chemical Society provides "Just Accepted" as a service to the research community to expedite the dissemination of scientific material as soon as possible after acceptance. "Just Accepted" manuscripts appear in full in PDF format accompanied by an HTML abstract. "Just Accepted" manuscripts have been fully peer reviewed, but should not be considered the official version of record. They are citable by the Digital Object Identifier (DOI®). "Just Accepted" is an optional service offered to authors. Therefore, the "Just Accepted" Web site may not include all articles that will be published in the journal. After a manuscript is technically edited and formatted, it will be removed from the "Just Accepted" Web site and published as an ASAP article. Note that technical editing may introduce minor changes to the manuscript text and/or graphics which could affect content, and all legal disclaimers and ethical guidelines that apply to the journal pertain. ACS cannot be held responsible for errors or consequences arising from the use of information contained in these "Just Accepted" manuscripts.



ACS Publications

is published by the American Chemical Society, 1155 Sixteenth Street N.W., Washington, DC 20036

Published by American Chemical Society. Copyright © American Chemical Society. However, no copyright claim is made to original U.S. Government works, or works produced by employees of any Commonwealth realm Crown government in the course of their duties.

Application of the Suzuki-Miyaura Reaction for the Postfunctionalization of the Benzo[4,5]thiazolo[3,2-*c*][1,3,5,2]oxadiazaborinine Core: An Approach towards Fluorescent Dyes

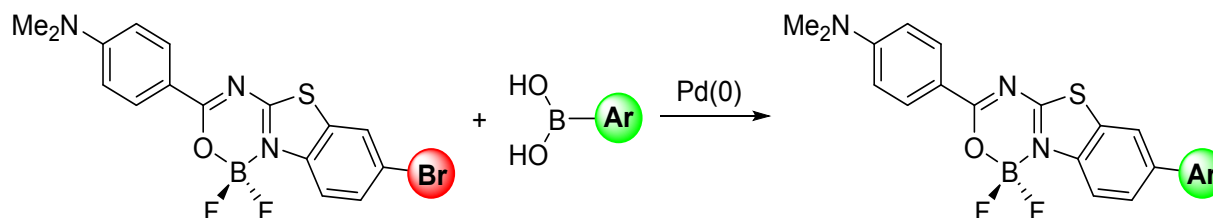
Mykhaylo A. Potopnyk,^{*,†} Dmytro Volyniuk,[‡] Roman Luboradzki,[#] Magdalena Ceborska,[#] Iryna Hladka,[‡] Yan Danyliv,[‡] and Juozas Vidas Gražulevičius^{*,‡}

[†]Institute of Organic Chemistry, Polish Academy of Sciences, Kasprzaka 44/52, 01-224, Warsaw, Poland, e-mail: potopnyk@gmail.com

[‡]Department of Polymer Chemistry and Technology, Kaunas University of Technology, Radvilenu pl. 19, LT-50254 Kaunas, Lithuania, e-mail: juozas.grazulevicius@ktu.lt

[#]Institute of Physical Chemistry, Polish Academy of Sciences, Kasprzaka 44/52, 01-224, Warsaw, Poland

Abstract:



Fluorescent dye based on 8-brominated benzo[4,5]thiazolo[3,2-*c*][1,3,5,2]oxadiazaborinine core was synthesized from benzo[*d*]thiazol-2-amine. The new boron complex can be effectively modified by palladium-catalyzed Suzuki-Miyaura cross-coupling reaction with (het)arylboronic acids. This reaction allows a valuable regioselective postfunctionalization of 1,3,5,2-oxadiazaborinine chromophores with different aromatic substituents. The solutions of obtained target complexes in organic solvents demonstrate high fluorescence quantum yields. Compound with 4-cyanophenyl groups at benzothiazole unit (Ar = 4-C₆H₄-CN) exhibits a comparatively high fluorescence quantum yield of 0.31 in the solid state.

Introduction

Fluorescent dyes play an extremely important role as functional materials for optoelectronic devices,¹ in supramolecular chemistry,² and biological imaging.³ Borondipyrromethenes (BODIPYs), due to high fluorescence efficiency of their solutions, are among the most extensively studied fluorescent dyes.⁴ However, BODIPYs usually exhibit low solid-state emission, caused by narrow Stokes shifts, which limits their applicability in optoelectronic devices.^{1c} Therefore, development of novel organoboron complexes, based on non-pyrrole ligands, with high

photoluminescence quantum yields in the solid state is an urgent task. Systematic studies of structure–properties relationship of such materials are critically important.

One of the promising classes of organoboron dyes is based on oxadiazaborinine ring.^{1c} Such dyes are synthesized by complexation of boron trifluoride with *N,O*-bidentate ligands, obtained by acylation of 2-amino-*N*-heterocycles. In the design of these complexes electron-poor nitrogen-containing heterocycles such as pyridine,⁵ pyrazine,^{5c,6} pyridazine,^{5c} 1,8-naphthyridine,⁷ or 1,3,4-thiadiazole⁸ were used as the *N*-coordinating centres. Recently, we have demonstrated that annulation of electrone-rich 1,3-thiazole⁹ and benzo[*d*]thiazole moieties¹⁰ to oxadiazaborinine enables to obtain the complexes exhibiting high fluorescence efficiency. Substituents in position 6 of benzo[*d*]thiazole unit affect photophysical properties of the complexes, depending of their donor/acceptor strength.¹⁰ Therefore, the further modification of such complexes is of great interest.

One of the most efficient method of expansion of π -conjugated systems is arylation.¹¹ In this context, Pd-catalyzed cross-coupling reaction plays the key role.¹² Arylation of BODIPY derivatives is widely investigated. It results in new fluorophores with interesting and practically useful structural and photophysical properties.¹³ In particular, Suzuki-Miyaura,¹⁴ Stille^{14d,15} reactions, as well as, direct C–H arylation¹⁶ were successfully used.

On the other hand, functionalized 1,3,5,2-oxadiazaborinine derivatives have been usually obtained from suitably functionalized ligands (prefunctionalization), followed by a complexation with boron trifluoride in the final step.^{5–8} Meanwhile, an introduction of the desired functional pattern in a later stage after the construction of the organoboron core (postfunctionalization) is much less explored.^{7d} Pd-catalyzed cross-coupling reactions as an instrument for the postfunctionalization of oxadiazaborinine derivatives are still unknown. Low stability of this class of complexes in the basic reaction medium apparently makes such transformations difficult.¹⁷

In this manuscript we describe the investigation of reactivity of bromo benzothiazolo-oxadiazaborinine analogue in Suzuki-Miyaura cross-coupling reaction with (het)arylboronic acids (Figure 1). To obtain the target complexes with different strength of acceptor and donor substituents, the corresponding boronic acids were selected. The influence of the selected substituents on photophysical properties of the complexes in solutions and in the solid state was investigated.

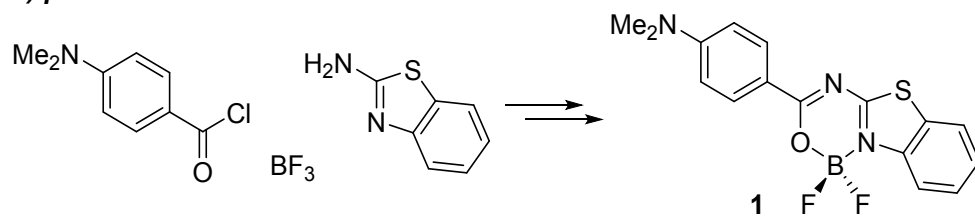
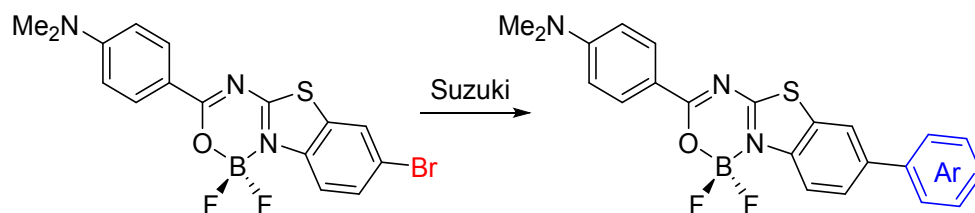
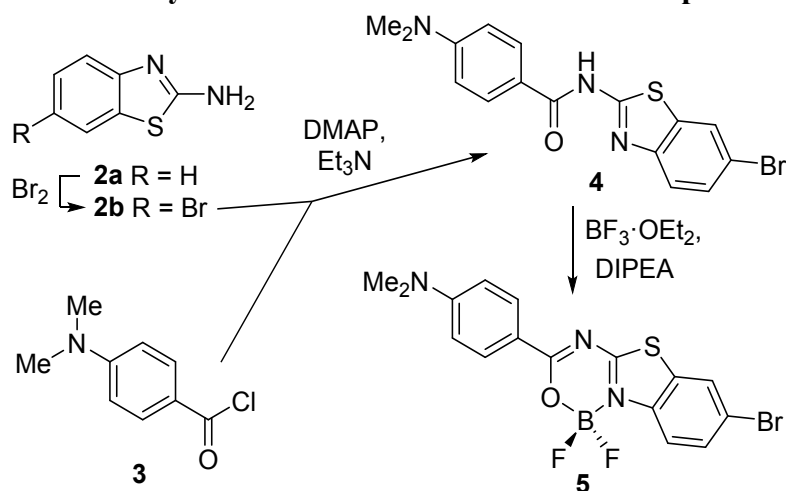
a) previous work**b) this work**

Figure 1. (a) Previous work: synthesis of benzo[*d*]thiazole-based BF₂-complexes, (b) modification of benzo[*d*]thiazolo-oxadiazaborinines via Suzuki-Miyaura reaction.

Results and Discussion**Synthesis and characterization.**

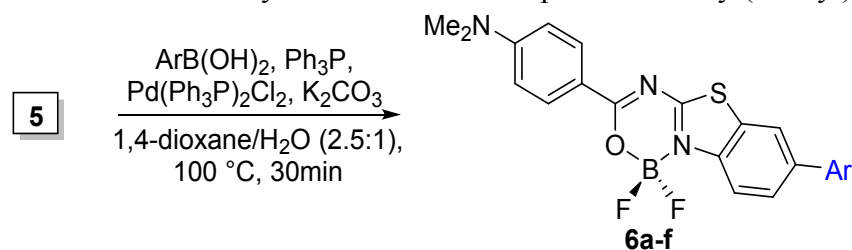
The preparation of necessary bromo benzothiazolo-oxadiazaborinine is presented in Scheme 1. The synthesis was started from commercially available benzo[*d*]thiazol-2-amine (**2a**), which was selectively brominated in glacial acetic acid medium in position 6 giving product **2b** in excellent yield (91%). To prepare the *N,O* ligands, 6-bromobenzo[*d*]thiazol-2-amine (**2b**) was acylated by (*para*-dimethylamino)benzoyl chloride (**3**) in the basic conditions in refluxing 1,4-dioxane to provide amide **4** in 65% yield. Compound **4** was treated with boron trifluoride diethyl etherate in the presence of *N,N*-diisopropylethylamine (DIPEA) to give benzothiazole-BF₂ complex **5** in good (74%) yield (Scheme 1).

Scheme 1. Synthesis of Benzothiazole-Boron Complex 5

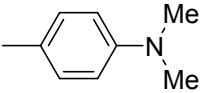
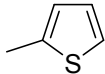


Such synthesized bromo derivative **5** was used in Suzuki-Miyaura cross-coupling reaction with aryl(thienyl)boronic acids. Pd(Ph₃P)₂Cl₂ was selected as an effective catalyst. The best yields (Table 1) were obtained when the molar ratio of bromo-substrate/boronic acid/Pd-catalyst was 1.00:1.50:0.05. The obtained complexes **6a–f** have different aromatic substituents at position 6 of benzo[*d*]thiazole unit, including electron-donor and electron-acceptor groups.

Table 1. Suzuki-Miyaura reaction of complex **5** with aryl(thienyl)boronic acid.



Compound	Ar	Yield, %
6a		89
6b		90
6c		84
6d		92

6e		97
6f		91

The characterization of all the synthesized compounds was performed by NMR (^1H , ^{13}C , ^{19}F) and IR spectroscopy, and high-resolution mass spectrometry. The solubility of complexes **6b**, **d**, **e** was too small to record ^{13}C NMR spectra of the satisfactory quality. Additionally, the structures of boron complexes **5** and **6a–f** were confirmed by single-crystal X-ray analysis (Figure 2, Figures S1–S8 and Tables S1–S7 in the Supporting Information).

X-ray Analysis.

Compound **5**, similarly to 6-unsubstituted benzothiazole analogue **1**,¹⁰ has near-to-planar solid-state geometry. The C5-C6-C9-N2 torsion angle is very small (around 1.5°). However, the incorporation of aryl substituent into the position 6 of benzothiazole moiety of the complex causes a twisting of the molecular skeleton. Interestingly, unlike the other complexes, the crystal packing of compound **6a** is formed by two symmetry independent molecules (**6a** and **6a-A** in Figure 2; Figures S1 and S2 in the Supporting Information). The first conformer (**6a**) shows a roughly planar molecular backbone with the C5-C6-C9-N2 and C16-C15-C17-C22 torsion angles of approximately 12.0° and -22.1° , respectively. In contrast, the second conformer (**6a-A**) demonstrates a bent conformation and the much smaller C5A-C6A-C9A-N2A and C16A-C15A-C17A-C22A torsion angles (-8.0° and 15.7°). In the case of compounds **6c–f** the absolute value of the C5-C6-C9-N2 torsion angle is small (from 0.8° to 6.5°), but unexpectedly increases to 13.5° in structure **6b**. On the other hand, the absolute value of the C16-C15-C17-C22 torsion angle of structures **6b–d** is in the range 23.3 – 33.9° , but decreases to 11.2° in the case of structure **6e**. Notably, the structure of complexes with five-membered thiophene substituent at the benzothiazole unit (**6f**) is much planar; the absolute value of the C16-C15-C17-C18 torsion angle is approximately 10.4° (Figure 2).

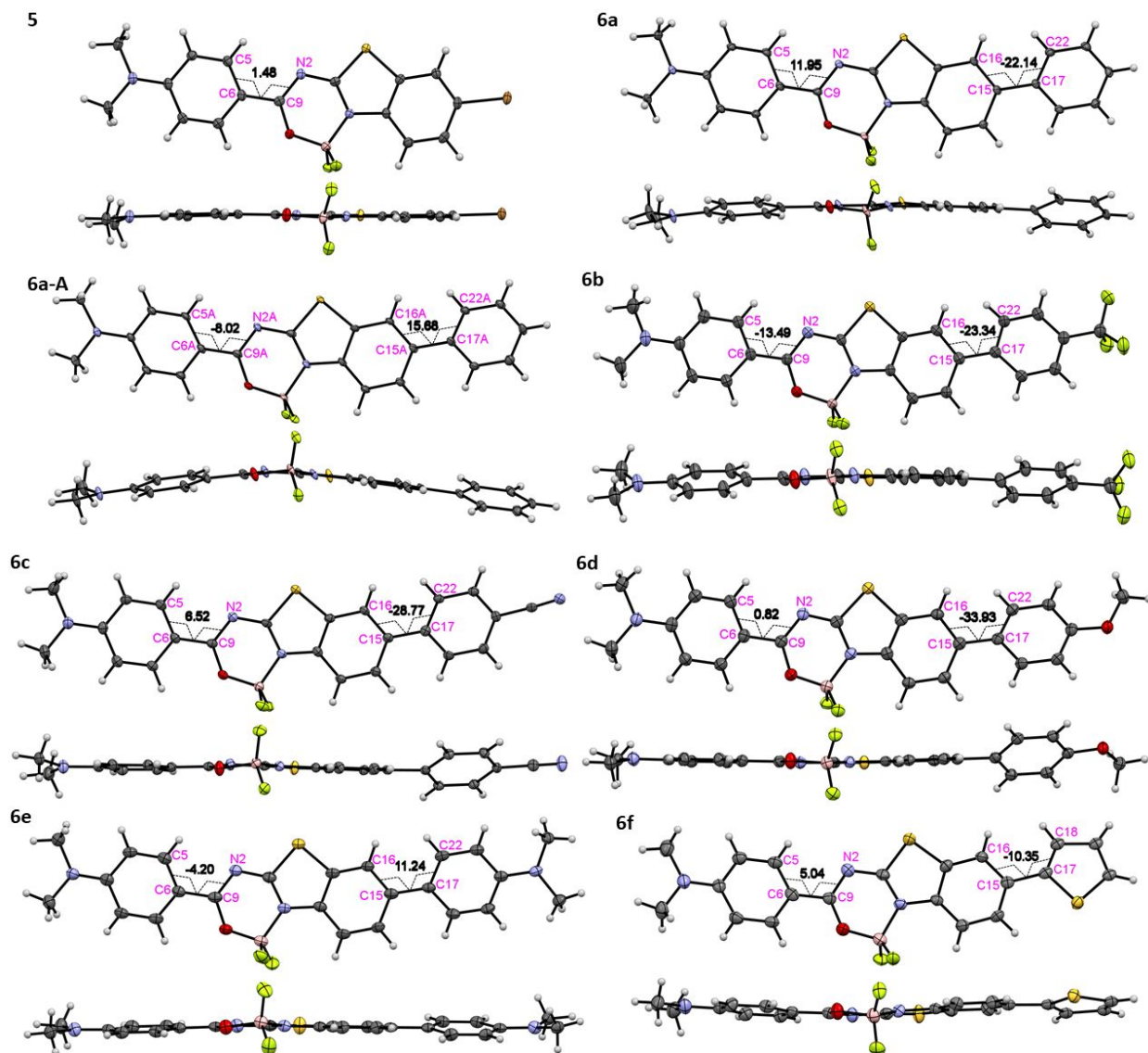


Figure 2. X-Ray structures of boron complexes **5** and **6a–f** (top and front views). The ellipsoid contour of probability level is 50%.

Complexes **5** and **6a,b** exhibit well-ordered molecular packing, characterized by a triclinic lattice with two (**5** and **6b**) or four (**6a**) molecules in unit cell and the space group *P*-1 (Tables S1–S3 in the Supporting Information). The packing of complex **5** is presented in Figure 3. In the top view the 2-D net structure is arranged through numerous intermolecular H-bonding interactions ($\text{CH}\cdots\text{F}$, $\text{CH}\cdots\text{Br}$, $\text{CH}\cdots\text{S}$), as well as, the S–F interaction. While, in the side and the front views, antiparallel oriented neighboring molecules **5** are connected by π – π /H– π interactions and hydrogen bonds, forming the stairs.

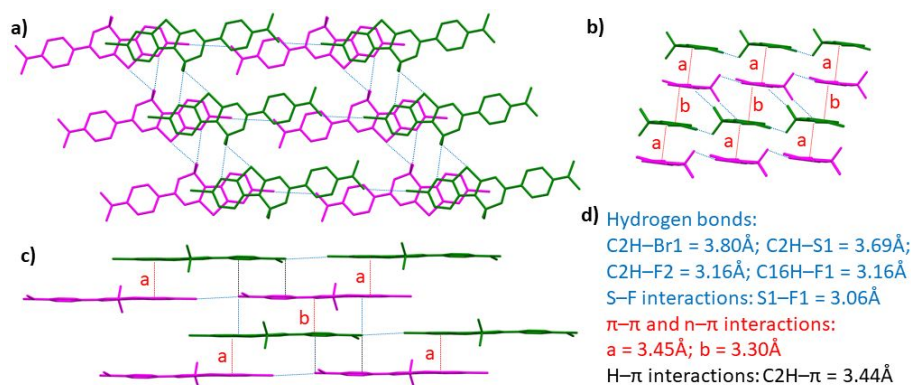


Figure 3. Molecular packing of complex **5**: (a) top view; (b) side view; (c) front view; (d) list of intermolecular interactions. Blue-dotted lines show hydrogen bonds and S–F interactions; red-dotted lines show $\pi-\pi/n-\pi$ interactions; black-dotted lines show H– π interactions.

Specific molecular packing is observed in the case of compound **6a**. Flat (green and magenta in Figure 4) and bent (orange and grey in Figure 4) conformations of this compound form layers in the side and front views. Inside the layer the single molecules are connected by several hydrogen bonds ($C1H-F2$, $C1H-O1$, $C1^AH-F1^A$, $C19^AH-F1^A$) and weak H– π interactions ($C16H-C21$). While the connection between the layers is stronger and realized by numerous intermolecular n– π and H– π interactions.

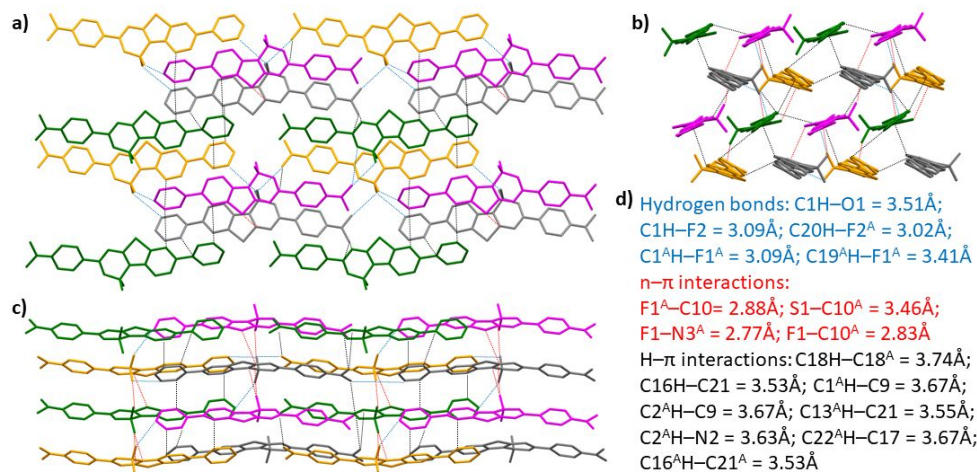


Figure 4. Molecular packing of complex **6a**: (a) top view; (b) side view; (c) front view; (d) list of intermolecular interactions. Blue-dotted lines show hydrogen bonds; red-dotted lines show n– π interactions; black-dotted lines show H– π interactions.

Molecules of complex with 4-(trifluoromethyl)phenyl substituent (**6b**) form a crystal packing characterized by "molecular stairs" (Figure 5), similarly to that of bromo-analogue **5**. However, in

this case, the twisting of both aryl substituents at the benzothiazolo-oxadiazaborinine moiety prevents the π - π interactions. As a results, hydrogen atoms from 4-(trifluoromethyl)phenyl group interact with aromatic π -electrons of neighboring molecules ($C18H-\pi = 3.27\text{\AA}$, $C21H-\pi = 3.32\text{\AA}$, distance between carbon atoms and aromatic planes). In the same time, the availability of five fluorine atoms from BF_2 and CF_3 groups promotes the formation of the strong n - π interactions ($F1-\pi = 2.84\text{\AA}$, $F5-\pi = 2.94\text{\AA}$, distance between aromatic planes and fluorine atoms), as well as hydrogen bonds ($C2H\cdots F3$, $C18\cdots F2$, $C16H\cdots F1$), and S-F/F-F interactions.

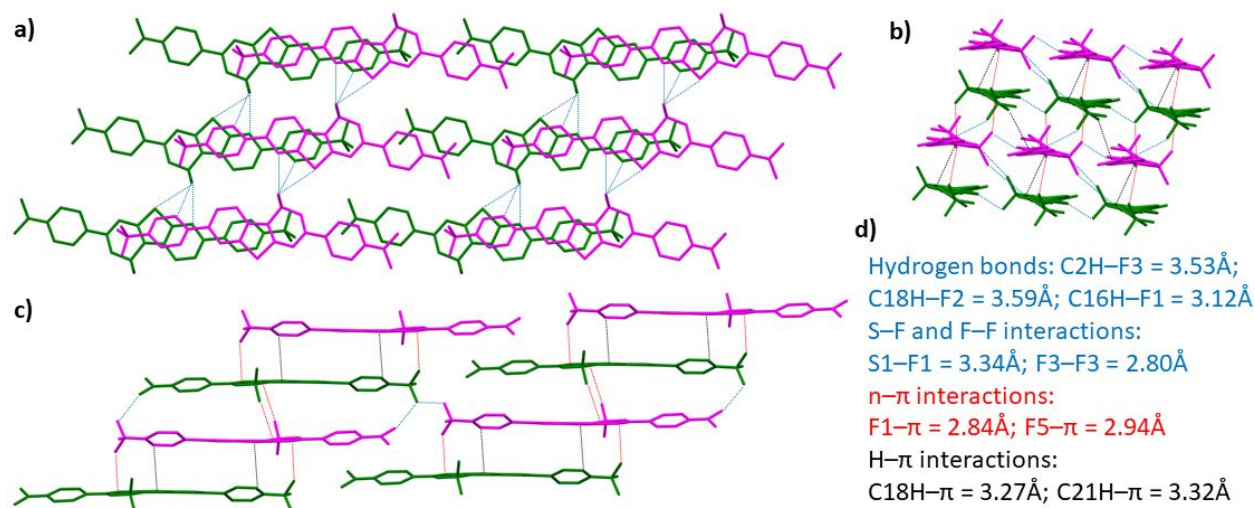


Figure 5. Molecular packing of complex **6b**: (a) top view; (b) side view; (c) front view; (d) list of intermolecular interactions. Blue-dotted lines show hydrogen bonds, S-F and F-F interactions; red-dotted lines show n - π interactions; black-dotted lines show H - π interactions.

Compounds **6c** and **6d** crystallize in a $P2_1/c$ monoclinic space group with four molecules in the asymmetric unit (Tables S4 and S5 in the Supporting Information). Specificity of molecular packing of complex **6c** (Figure 6) is formation of dimers by "head-to-tail" orientated molecules, which are connected by weak π - π interaction ($a = 3.88\text{ \AA}$) between the benzothiazolo-oxadiazaborinine moieties of each, and two pairs of hydrogen bonds ($C16H\cdots F2$ and $C1H\cdots N4$). The neighboring parallel dimers are connected by π - π interaction ($b = 3.52\text{ \AA}$), H - π interactions between CH_3 group and twisted benzene ring (3.69 \AA), and double $C5H-F$ hydrogen bonds (3.07 \AA), and are shifted to each other, forming stairs. The neighboring stairs are connected by double $C19H-N4$ hydrogen bonds (3.31 \AA), creating the molecular monolayers, which in turn are connected by numerous hydrogen bonds ($C22H\cdots F1$; $C7H\cdots F2$; $C21H\cdots N2$; $C14H\cdots N4$), S-F and n - π interactions, forming a net-type structure (side view). Interestingly, inside these

monolayers the orientation of the single molecule planes is perpendicular to the plane of the layer, while the molecules from the neighboring monolayers are oriented at angle about 82° to each other.

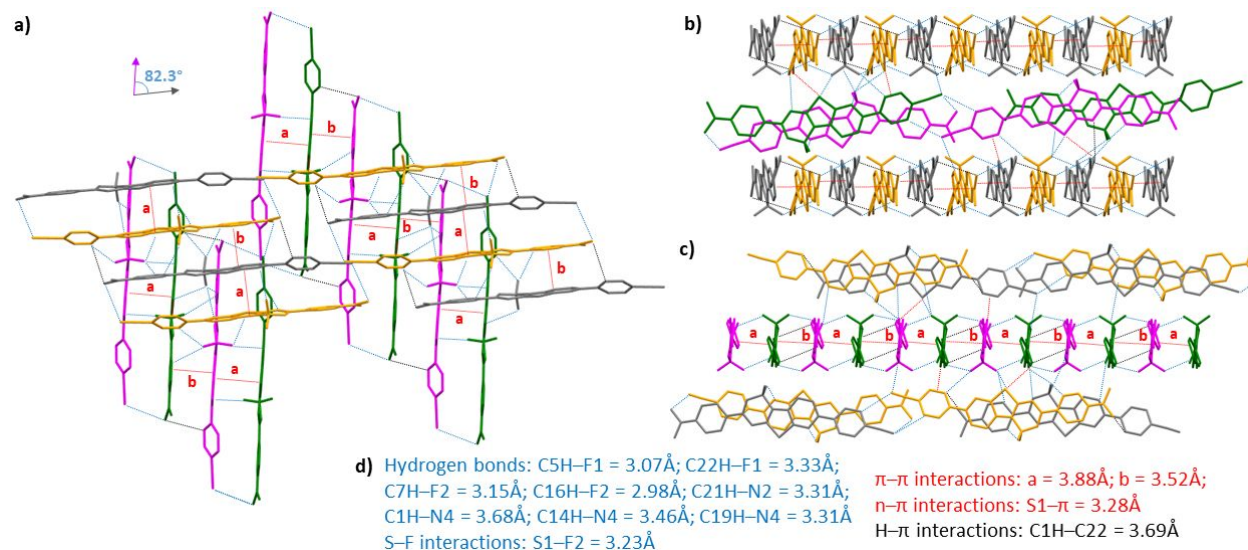


Figure 6. Molecular packing of complex **6c**: (a) top view; (b) side view; (c) front view; (d) list of intermolecular interactions. Blue-dotted lines show hydrogen bonds and S-F interactions; red-dotted lines show π - π /n- π interactions; black-dotted lines show H- π interactions.

Crystal packing of dye **6d** (Figure 7) is characterized by stacking columns. Inside these columns the molecules are antiparallel oriented and connected to each other by π - π /n- π interactions ($a = 3.50$ Å) between planes of 4-(benzo[4,5]thiazolo[3,2-*c*][1,3,5,2]-oxadiazaborinin-3-yl)-*N,N*-dimethylaniline core, as well as, by H- π interaction between NCH_3 group and benzothiazole moiety ($\text{C2H}-\pi = 3.38$ and $\text{C2H}-\pi' = 3.62$ Å). The connection between the stacking columns occurs by numerous hydrogen bonds ($\text{C2H}\cdots\text{O2}$; $\text{C1H}\cdots\text{F1}$; $\text{C16H}\cdots\text{F1}$; $\text{C16H}\cdots\text{F2}$), S1-F2 and C23H- π interactions. In the side view the columns are oriented parallel. While in the front view the angle between the neighboring columns is being 166.3° .

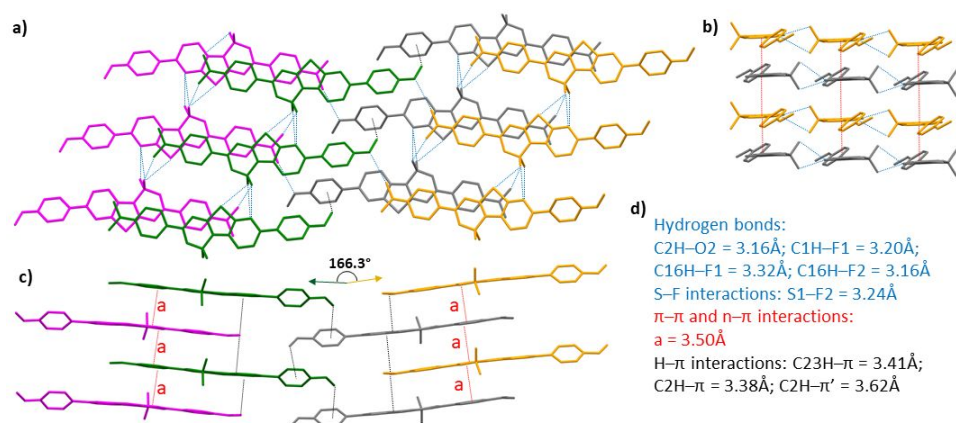


Figure 7. Molecular packing of complex **6d**: (a) top view; (b) side view; (c) front view; (d) list of intermolecular interactions. Blue-dotted lines show hydrogen bonds and S-F interactions; red-dotted lines show π - π and n- π interactions; black-dotted lines show H- π interactions.

Complexes **6e** and **6f** exhibit well-ordered molecular packing, characterized by an orthorhombic lattice with four molecules per unit cell and the space group $P2_12_12_1$ (Tables S6 and S7 in the Supporting Information). Coplanar molecules **6e** form the stairs (painted in the same colour in Figure 8), which are clearly visible in the side view. The angle between the planes of neighboring molecules is 66.8° (Figure 8b). These neighboring molecules are oriented "head-to-tail" and connected to each other by C23H- π interactions and a series of hydrogen bonds (C13H...N4, C24H...F1, C23H...S1, and C24H...S1) between benzo[4,5]thiazolo[3,2-*c*][1,3,5,2]oxadiazaborinine unit and dimethylamino group from the benzothiazole side. Notably, this coordinated interaction between 7-(4-dimethylaminophenyl)benzo[4,5]thiazolo[3,2-*c*][1,3,5,2]oxadiazaborinine moieties promotes the relative planarity of the molecular scaffold (see the unexpectedly small C16-C15-C17-C22 torsion angle of this molecule in Figure 2). On the other hand, the 4-dimethylaminophenyl group at the oxadiazaborinine side induces the C8H- π interactions with the analogical group of the neighboring molecules (interaction between grey and green molecules in Figures 8a and 8c). Perpendicular to the stairs the molecules **6e** run along zig-zag chains at the 161.1° angle as seen in the top (green and orange molecules in Figure 8a) and the front (magenta and grey molecules in Figure 8c) views.

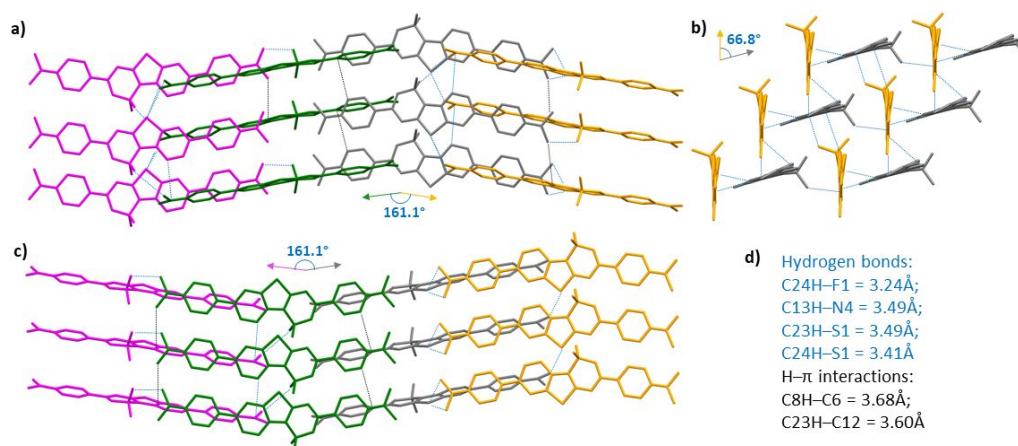


Figure 8. Molecular packing of complex **6e**: (a) top view; (b) side view; (c) front view; (d) list of intermolecular interactions. Blue-dotted lines show hydrogen bonds; black-dotted lines show H- π interactions.

Similarly, molecules **6f** build the zig-zag chains in the top and the front views and the stairs in the side view (Figure 9). In this case, the angle between the molecules formed zig-zag chains is approximately 160°. Inside the stairs the molecules are connected to each other by F2- π interactions. The 7-(thiophen-2-yl)benzo[4,5]thiazolo[3,2-*c*][1,3,5,2]oxadiazaborinine moieties participate in the formation of C20H...F1 hydrogen bonds, S1- π , C13H- π and C18H- π interactions with analogical part of the neighboring molecules, located at the 78.8° angle (Figure 9b). The 4-dimethylaminophenyl groups are connected to each other by C4H- π and C8H- π interactions (between grey and green molecules in Figures 9a and 9c).

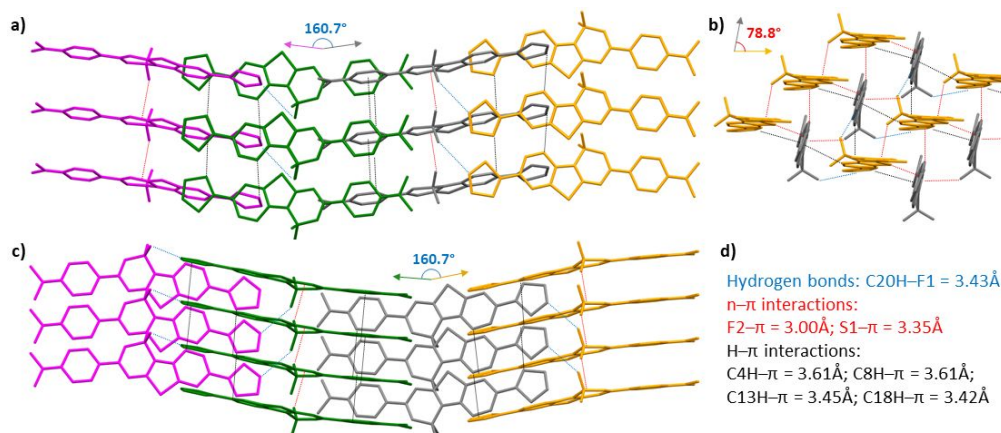


Figure 9. Molecular packing of complex **6f**: (a) top view; (b) side view; (c) front view; (d) list of intermolecular interactions. Blue-dotted lines show hydrogen bonds; red-dotted lines show n- π interactions; black-dotted lines show H- π interactions.

Photophysical Properties of the Solutions

The absorption and emission properties of complexes **5** and **6a-f** were measured as the dilute solution in five organic solvents (toluene, dichloromethane, tetrahydrofuran, acetone and acetonitrile). The corresponding normalized spectra are demonstrated in Figure 10; the spectroscopic data are summarized in Table 2.

The solutions of the studied complexes exhibit single absorption band in the violet-blue region of the spectrum and demonstrate almost no changes with the variation of solvent polarity. The absorption wavelength maxima (λ_{abs}) are located in the range of 427–431 nm for bromo derivative **5** and in the range of 430–439 nm for complexes **6a-f**, which are characterized by high molar absorption coefficients ($\epsilon = 64800\text{--}89000\text{ M}^{-1}\text{cm}^{-1}$). The absorbance curves of the complexes are unsymmetrical with a slight hypsochromic shoulder. The shoulder is the most clearly observed for compounds **6d** and **6f** in non-polar media; it is apparently induced by vibrational transition and disappeared in polar solvents due to the solvation effect.¹⁸

The comparing of these results with the previously reported for unsubstituted benzothiazole derivative **1** ($\lambda_{\text{abs}} = 421\text{--}425\text{ nm}$, $\epsilon = 53800\text{--}77300\text{ M}^{-1}\text{cm}^{-1}$ in different solvents)¹⁰ demonstrates that the incorporation of bromo (complex **5**) or aryl (complexes **6a-f**) substituents in position 6 of benzo[*d*]thiazole unit causes a bathochromic shift of the absorption bands and a slight increase of molar absorption coefficient.

The dilute solutions of complexes **5**, **6a-d,f** demonstrate also single emission bands. The small bathochromic shoulder is observed in the emission spectra of the solutions of compounds **6d** and **6f** in toluene, which is in agreement with the corresponding observation in absorption spectra.

The emission wavelength maxima (λ_{em}) of the solutions of bromobenzothiazole complex **5** are very similar to those of unsubstituted benzothiazole derivative **1**.¹⁰ In toluene it is located at 450 nm while the corresponding parameters of the toluene solutions of **6a-d,f** are observed in the range of 457–462 nm. Bathochromic shifts of the emission maxima by 29–36 nm (1294–1646 cm^{-1}) are observed for the solutions of the studied compounds upon changing the solvent from toluene to acetonitrile (Figure 10, Table 2). The positive solvatofluorochromism of the solutions of complexes **5**, **6a-d,f** results in the corresponding growth of the Stokes shifts ($\Delta\nu = \nu_{\text{abs}} - \nu_{\text{em}}$) with

the increase of solvent polarity (Table 2). It indicates that the emissions of these compounds are partially or fully induced by intramolecular charge transfer (ICT) state. To quantify the ICT character of the studied compounds, the Lippert-Magata analysis was carried out. The plots of Stokes shifts versus orientation polarizability of the solvents (Δf) are shown in Figures S9–S15 in the Supporting information. The slopes of the Lippert-Mataga plots were found to be in the range from 4162 to 5189 cm^{-1} demonstrating that differences in dipole moments of the studied complexes are in order of **6d** < **6f** < **6a** < **5** < **6b** < **6c** (Figures S9–S13, S15 in the Supporting information). This regularity correlates very well with donor/acceptor strength of the substituents at position 6 of benzo[d]thiazole unit of the corresponding compounds.

Fluorescence quantum yield (Φ) of bromobenzothiazole complex **5** (Table 2) is lower than that of unsubstituted analogue **1** ($\Phi = 0.84$ for toluene solution, 0.77 for DCM solution, 0.78 for THF solution, 0.31 for acetone solution, and 0.17 for acetonitrile solution).¹⁰ This observation can be explained by "heavy atom effect". The values of fluorescent quantum yield of the solutions of dyes **6a–d, f** in non-polar solvents are very high ($\Phi = 0.80$ – 0.99 for the solutions in toluene, Table 2), but they considerably decrease with increasing solvent polarity ($\Phi = 0.29$ – 0.44 for the solutions in acetonitrile). This smallest decrease is observed for the solutions of compounds with donor (het)aryl (4-methoxyphenyl or 2-thienyl) substituents at the benzothiazole moiety ($\Phi = 0.43$ and 0.44).

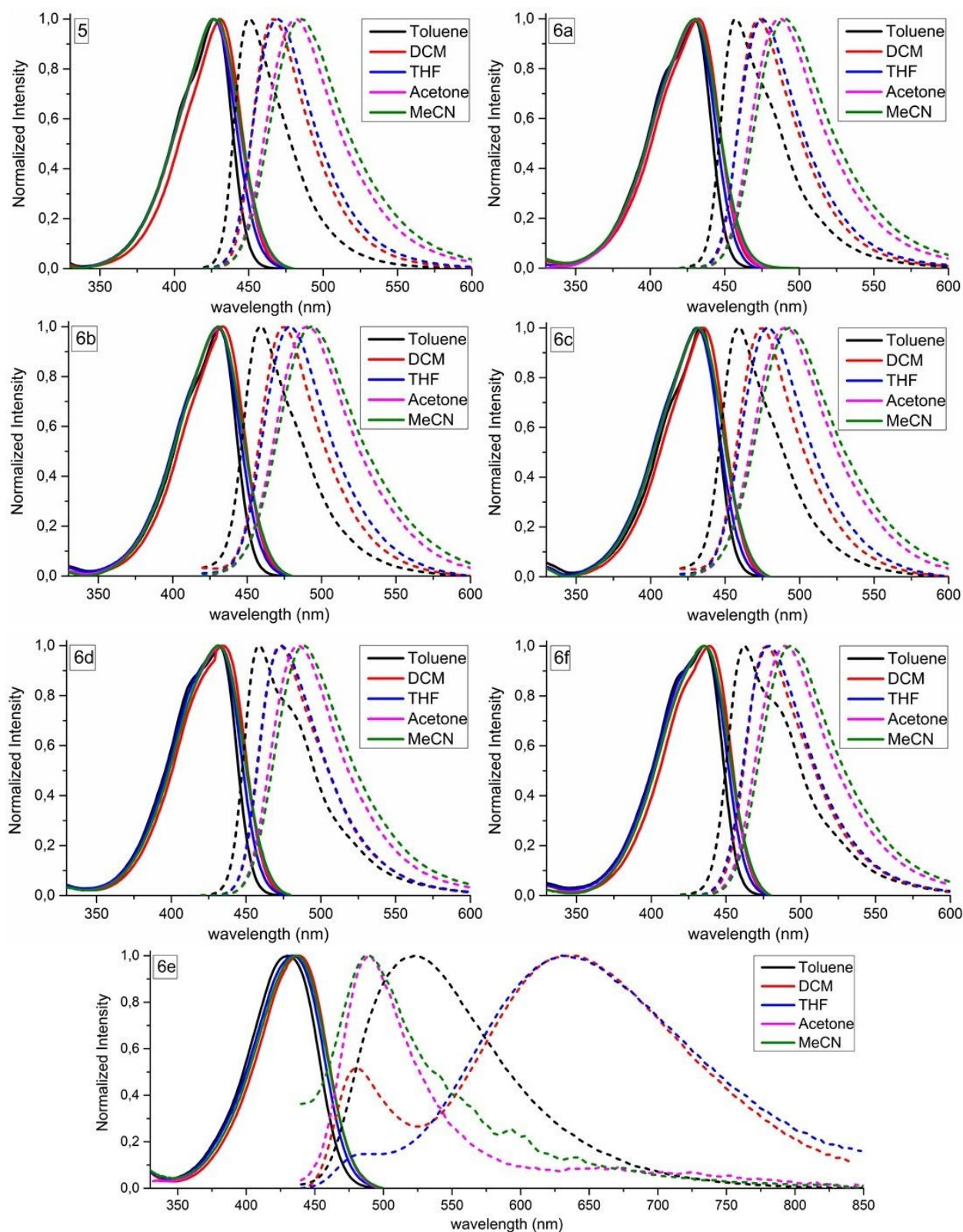


Figure 10. Absorption (solid lines) and emission (dashed lines) spectra of the solutions of complexes **5** and **6a-f** in toluene (black), DCM (red), THF (blue), acetone (magenta), and MeCN (olive) ($\lambda_{\text{ex}} = 350$ nm).

Table 2. Photophysical properties of the solutions complexes **5** and **6a–f** in different solvents.

Compound	Solvent	λ_{abs} , nm	ϵ , $\text{M}^{-1}\text{cm}^{-1}$	λ_{em} , nm	$\Delta\nu$, cm^{-1}	Φ	B^a , $\text{M}^{-1}\text{cm}^{-1}$
1	toluene	421	62600	450	1531	0.84	52600
	DCM	425	77300	467	2116	0.77	59600
	THF	424	70200	469	2263	0.78	54700
	acetone	425	74900	482	2782	0.31	23200
	acetonitrile	421	53800	486	3177	0.17	9100
5	toluene	427	66700	450	1197	0.74	49400
	DCM	431	85500	467	1789	0.61	52200
	THF	426	71300	469	2152	0.55	39200
	acetone	427	76500	482	2672	0.27	20700
	acetonitrile	430	81200	486	2680	0.13	10600
6a	toluene	430	78100	457	1373	0.92	71900
	DCM	432	86200	473	2006	0.75	64700
	THF	430	79400	475	2203	0.82	65100
	acetone	430	76200	487	2722	0.56	42700
	acetonitrile	430	76900	491	2889	0.33	25400
6b	toluene	431	69500	459	1415	0.80	55600
	DCM	434	68300	475	1989	0.74	50500
	THF	430	68200	479	2379	0.75	51200
	acetone	430	76700	490	2848	0.42	32200
	acetonitrile	430	76000	493	2971	0.29	22000
6c	toluene	434	89000	459	1255	0.99	88100
	DCM	436	82300	475	1883	0.98	80700
	THF	431	70800	479	2325	0.96	68000
	acetone	432	75900	490	2740	0.55	41700
	acetonitrile	432	83800	493	2864	0.32	26800
6d	toluene	431	70900	459	1415	0.95	67300
	DCM	437	78500	473	1742	0.79	62000
	THF	431	81300	474	2104	0.82	66700
	acetone	432	75300	485	2530	0.65	48900
	acetonitrile	431	64900	488	2710	0.43	27900
6e	toluene	430	64800	523	4135	0.78	50500
	DCM	438	72700	480/631	1998/6983	0.04	2900
	THF	433	75600	487/630	2561/7221	0.03	2300
	acetone	436	65500	490	2527	0.01	700
	acetonitrile	435	64900	487	2454	0.02	1300
6f	toluene	436	73600	462	1291	0.84	61800
	DCM	439	76300	477	1815	0.91	69500
	THF	436	72500	478	2015	0.87	63100
	acetone	435	67800	489	2539	0.65	44100
	acetonitrile	435	79900	493	2705	0.44	35100

^a $B = \epsilon \times \Phi$

The totally different behaviour was observed for complex **6e**. The emission spectrum of its toluene solution has a single broad peak in the blue-green region with the intensity maximum at 523 nm. The main emission peak of the solutions in DCM and THF is bathochromically shifted ($\lambda_{em} \sim 630$ nm). Additionally, the low intensity emission peak at 480–487 nm is also present in the higher-energy region. Excitation spectra at emission wavelengths of 487 nm and 630 nm were recorded for THF and DCM solutions of compound **6e** (Figure S16). The absorbance band and excitation spectra at emission wavelengths of 487 nm and 630 nm was found at the same wavelengths meaning that compound **6e** (in whole) is responsible for emission in high-energy and low-energy regions (Figure 10). It additionally proves that the dual emission of the solutions of **6e** in DCM and THF is not related to different compounds. Intensities of the high-energy and low-energy emission bands are very dependent on polarity of the media in which that emitter **6e** is dispersed. The solutions of compound **6e** in acetone and acetonitrile exhibit blue shifted peaks located at 487–490 nm. Thus, fluorescence spectrum of the solution of complex **6e** in non-polar toluene exhibits emission with large Stokes shift (4135 cm^{-1}), whereas emission with the maximum at *ca.* 480–490 nm appears, and Stokes shift decreases as the solvent polarity is increased (Figure 10).

To explore the nature of dual emission of complex **6e**, the Lippert-Mataga plot was also performed (Figure S14 in the Supporting information). Two fitted lines were obtained for the Stokes shift values corresponded both the high- and low-energy emissions. Through the analysis of the fitted line in the "high-energy region", a low slope value (1938 cm^{-1}) was obtained. While the fitted line in "low-energy region" has a much higher slope value (14694 cm^{-1}). These observations indicate, that both the high- and low-energy emission bands are most probably related to ICT nature since they are sensitive to solvent polarity. The high-energy emission band of complex **6e** is apparently related to ICT from donating (*N,N*-dimethylamino)phenyl group, attached directly to 1,3,5,2-oxadiazaborinine ring, to accepting benzo[4,5]thiazolo[3,2-*c*][1,3,5,2]oxadiazaborinine moiety, similarly to emission of complexes **5**, **6a–d,f** (Figure 10). Whereas the low-energy emission band of dye **6e** should be related to intramolecular charge transfer (ICT*) from (*N,N*-dimethylamino)phenyl donor substituent at position 6 of benzo[*d*]thiazole unit to benzo[4,5]thiazolo[3,2-*c*][1,3,5,2]oxadiazaborinine acceptor. Thereby, we assume that emission of complex **6e** origins from both ICT and ICT* emissive excited states.

Fluorescence efficiency of the solution of compound **6e** in toluene is high ($\Phi = 0.78$), however, in the other solvents the emission is almost completely quenched ($\Phi = 0.01$ – 0.04 for the solutions in DCM, THF, acetone, and acetonitrile). These results indicate that, due to the high ICT* effect, the decrease of the fluorescence quantum yield of the solutions of complex **6e** with the increase of solvent polarity is much higher, than in the case of complexes **6a–d,f** (Table 2).

To better assess the relative brightness of investigated fluorescent dyes, molecular fluorescence brightness (B , the product of the molar absorption coefficient and the fluorescent quantum yield) was calculated (Table 2). The highest value of fluorescence brightness was obtained for toluene solution of complex **6c** ($B = 88100 \text{ M}^{-1}\text{cm}^{-1}$).

The excited-state lifetimes (τ) of the solutions of complexes **5**, **6a–f** in toluene were measured (Table S8 and Figures S25–S31 in the Supporting Information). They ranged from 1.31 to 1.96 ns.

Electrochemical Properties

Electrochemical properties of the solutions of complexes **5** and **6a–f** in dichloromethane were studied by cyclic voltammetry at a voltage scan rate of 100 mV/s, using 0.1 M Bu_4NPF_6 as supporting electrolyte and ferrocene as the internal standard. Cyclic voltammograms are shown in Figures S17–S23 in the Supporting Information.

The values of ionization potentials (IPs) and electron affinities (EAs) were estimated by the following equations: $\text{IP} = E_{\text{ox}}^{\text{onset}} + 4.4$ and $\text{EA} = E_{\text{red}}^{\text{onset}} + 4.4$, where $E_{\text{ox}}^{\text{onset}}$ is the onset oxidation potential and $E_{\text{red}}^{\text{onset}}$ is the onset reduction potential (Table 3). IPs of complexes **5**, **6a–d** were found to be comparable (5.10–5.13 eV), which indicate the similar HOMO energy level of the molecules. However, IPs value of compound **6e** was found to be considerably lower (4.64 eV). Cyclic voltammogram of complex **6f** demonstrated two oxidative peaks, which correspond to ionization potentials of 4.84 and 5.00 eV (Table 3). EA values of complexes **5**, **6a–e** ranged from 2.37 to 2.52 eV. EA of compound with thiophene substituent (**6f**) was found to be significantly higher (2.88 eV).

Table 3. Onset Oxidation and Onset Reduction Potentials, Ionization Potentials and Electron Affinities of Compounds **5 and **6a–f****

Compound	$E_{\text{ox}}^{\text{onset}}$, V	$E_{\text{red}}^{\text{onset}}$, V	IP, eV	EA, eV
5	0.71	-1.90	5.11	2.50
6a	0.71	-1.94	5.11	2.46
6b	0.70	-1.91	5.10	2.49
6c	0.73	-1.88	5.13	2.52
6d	0.70	-2.03	5.10	2.37
6e	0.24	-1.95	4.64	2.45
6f	0.44/0.60	-1.52	4.84/5.00	2.88

Quantum Chemical Calculations

To gain a better understanding of the photophysical properties of the investigated benzothiazole boron complexes, density functional theory (DFT) and time-dependent DFT (TD-DFT) computational studies were performed using the Gaussian 09 software package.²⁰ Geometrical structures of the investigated complexes were optimized, and the molecular energy levels were calculated at the B3LYP functional and 6-31G* basis set with the addition of dichloromethane solvent effect utilizing the integral-equation-formalism polarizable continuum model (IEFPCM).

Analogically to the X-ray data, theoretically optimized structure of complex **5** has a planar geometry. In the case of compounds **6a–f** the aryl(thienyl) substituents at benzothiazole unit are twisted with respect of plane of the rest of molecules due to the intramolecular interaction of *ortho*-hydrogen atoms. As a result, this steric effect induces weakening of the π -conjugation between the twisted parts of molecules **6a–f**.

The DFT-calculated frontier molecular orbitals (HOMO-1, HOMO, LUMO, and LUMO+1) are shown in Figure 11. Similarly to compound **1**,¹⁰ the HOMOs of compounds **5** and **6a–d,f** are somewhat more localized on the the (*N,N*-dimethylamino)phenyl group due to the strong electron donating effect of this unit; whereas the LUMOs are delocalized along 3-(4-dimethylaminophenyl)-benzo[4,5]thiazolo[3,2-*c*][1,3,5,2]oxadiazaborinine scaffold. This observation confirms the ICT character of fluorescence of these compounds.

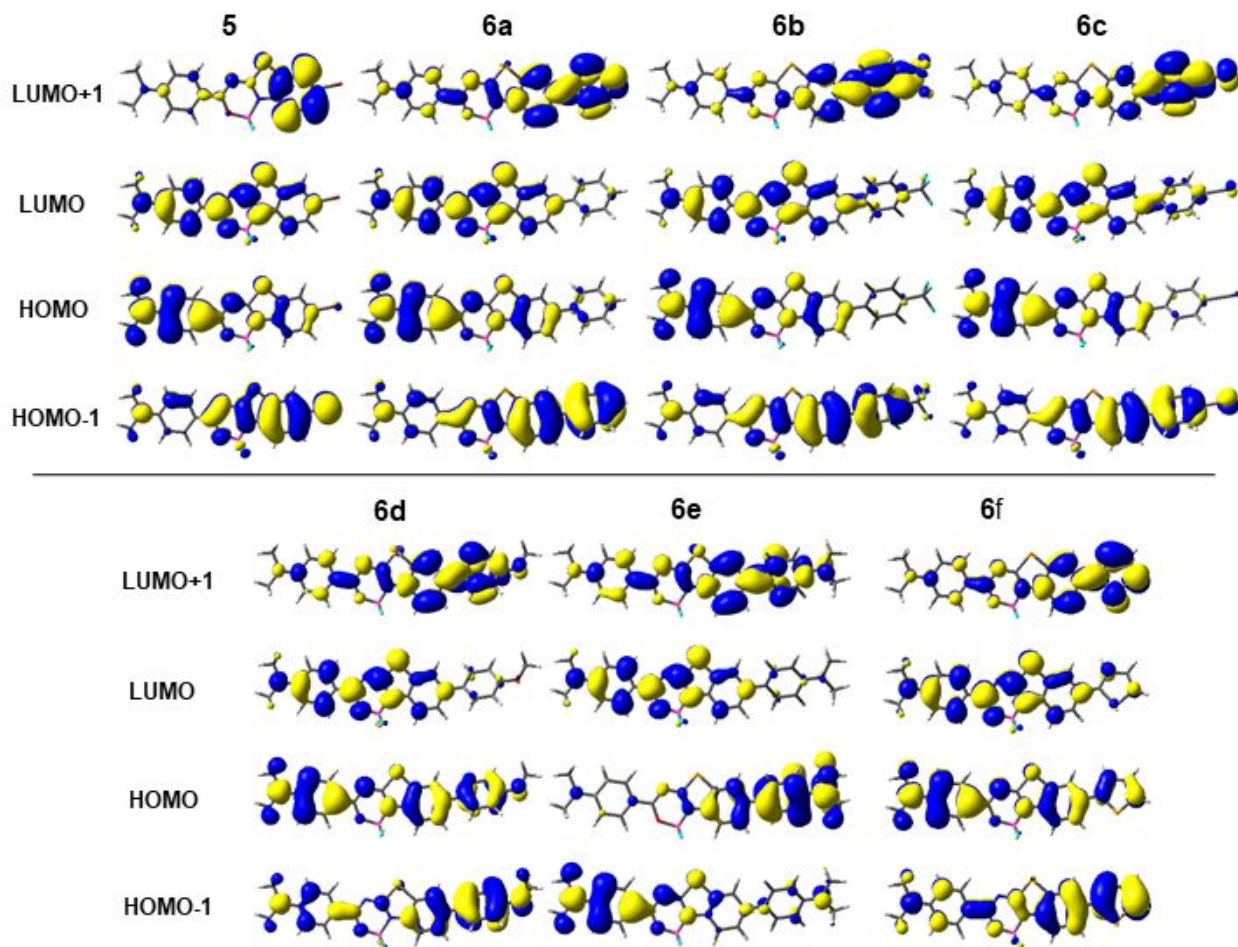


Figure 11. Frontier molecular orbitals of compounds **5** and **6a–f**.

The comparison of molecular orbital distribution on aryl substituents at benzothiazole unit shows that phenyl, 4-(trifluoromethyl)phenyl and 4-cyanophenyl groups (compounds **6a–c**) take a small part in both the HOMO and LUMO distribution. On the other hand, the donor substituents also make a small influence on LUMO, however, they definitely have a greater impact on HOMO distribution. Delocalization of HOMO density on 4-methoxyphenyl and 2-thienyl substituents in molecules **6d** and **6f**, respectively, results in the decrease of ICT character of emission of these complexes, which is in good agreement with the decreasing of the corresponding slope values of the Lippert-Mataga plots (Figures S9–S13, S15 in the Supporting information). HOMO electron density of complex **6e** is shifted to (*N,N*-dimethylamino)phenyl group attached to benzothiazole unit, while the HOMO-1 of this molecule has profile similar to the HOMO of compounds **5** and **6a–d,f**.

The theoretically calculated excitation energies for the six lowest singlet excited states, maximum absorption wavelengths (λ_{max}), oscillator strengths (f), and molecular contribution of the leading configurations (Table S9 in the Supporting Information) were obtained using TD-DFT computations. The analysis of TD-DFT results indicates that excitations of complexes **5** and **6a–d,f** preferably are going on first singlet excited state ($S_0 \rightarrow S_1$, $f = 1.50\text{--}1.76$, $\lambda_{\text{max}} = 429\text{--}449$ nm), when electrons move from HOMO to LUMO. However, in the case of compound **6e**, the excitation predominantly occurs on the second singlet excited state ($S_0 \rightarrow S_2$, $f = 1.22$, $\lambda_{\text{max}} = 418$ nm), which corresponds to the transition of electron from the HOMO-1 to the LUMO. De-excitation of molecule **6e** should include two steps. In the first step, the transition of electron from HOMO to HOMO-1 forms relatively stable zwitter-ion with the negative charge on the twisted 4-dimethylaminophenyl group and the positive charge on the 7-(4-dimethylaminophenyl)benzo[4,5]thiazolo[3,2-*c*][1,3,5,2]oxadiazaborinine moiety; the second step includes transition of another electron from LUMO to HOMO.

Solid-State Fluorescence Properties of Complexes **6a–f**

The normalized fluorescence spectra of the solid films of complexes **6a–f** are shown in Figure 12. The corresponding spectrum of unsubstituted compound **1** and bromo derivative **5**, as well as, the spectroscopic data are summarized in the Supporting Information (Figure S24 and Table S10). The emission maxima of the studied compounds in the solid state are bathochromically shifted relative to those of the corresponding dilute solutions. Compounds **6a–d,f** demonstrate similar solid-state emission bands, whereas complex **6e** with 4-dimethylaminophenyl substituents at benzothiazole unit is characterized by wider fluorescence bands (Figure 12). This confrontation is analogical to those for the toluene solutions (Figure 10). Thereby, we assume that solid-state emission of complex **6e** mainly originated from ICT* state, in contrast to the solid-state emissions of dyes **6a–d,f**, mainly originated from ICT state.

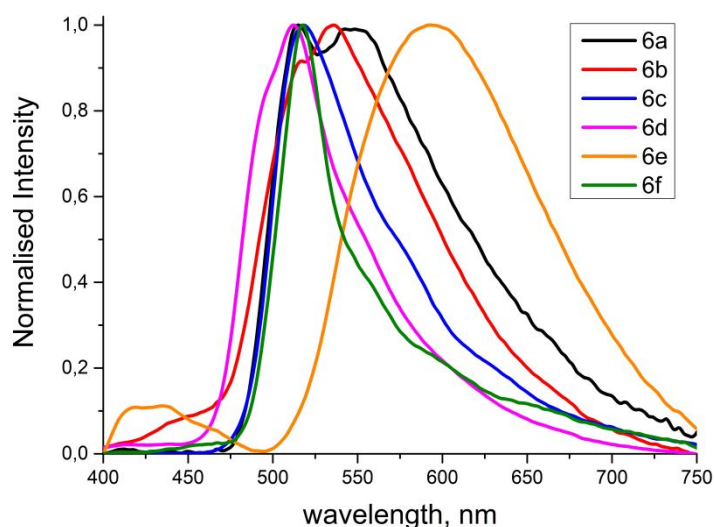


Figure 12. Normalized solid-state emission spectra of complexes **6a–f** ($\lambda_{\text{ex}} = 350$ nm).

Most of the investigated complexes exhibit weak solid-state fluorescence ($\Phi_{\text{solid}} = 0.02$ for complex **5**, and 0.06–0.17 for aryl-substituted analogous **6a,b,d–f**), which is apparently a result of an aggregation-induced quenching (AIQ) due to the dense molecular packing (Figures 3–5, 7–9). In contrast, the solid-state fluorescence quantum yield of boron complex **6c** is relatively high ($\Phi_{\text{solid}} = 0.31$). This observation can apparently be explained by decrease of AIQ, caused by the specificity of the molecular packing of this compound (Figure 6). In this case the π – π and H– π interactions between the molecules are weaker, compared to those taking place in complexes **6a,b,d–f**. The presence of nitrile group in molecule **6c** promotes the formation of additional hydrogen bonds.

Conclusions

To conclude, three-step synthesis of new fluorescent dye **5** based on 8-brominated benzo[4,5]thiazolo[3,2-*c*][1,3,5,2]oxadiazaborinine core was performed, starting from benzo[*d*]thiazol-2-amine. Complex **5** was successfully modified by the Suzuki-Miyaura cross-coupling reaction with aryl(thienyl)boronic acids, to obtain compounds **6a–f** with different aromatic substituents at position 6 of benzo[*d*]thiazol moiety, including electron-donating and electron-withdrawing groups. The structural and photophysical properties of the synthesized oxadiazaborinine derivative were studied. The solutions of the obtained complexes in non-polar solvents demonstrated very high fluorescence quantum yields in nonpolar solvents. Lower efficiencies of emission of the solutions in polar solvents is explained by intramolecular charge

transfer. Attachment of (*N,N*-dimethylamino)phenyl group at benzothiazole unit caused specific photophysical properties, which are related to the high ICT* effect. Compound with 4-cyanophenyl substituent at benzothiazole unit exhibited a comparatively high fluorescence quantum yield in the solid state ($\Phi_{\text{solid}} = 0.31$).

Experimental Section

General

All reagent-grade chemicals [including benzo[*d*]thiazol-2-amine (**2a**), (*para*-dimethylamino)benzoyl chloride (**3**), arylboronic acids] and solvents were received from commercial sources (TCI, Aldrich, Alfa Aesar, or Acros Organics) and used without further purification. Column chromatography was performed on silica gel (Merck, 230-400 mesh). Melting points of all synthesized compounds were measured on Automatic Melting Point System (OptiMelt, Stanford Research Systems). The NMR spectra were recorded with Bruker Avance II 400 MHz (at 400 MHz, 100 MHz, and 375 MHz for ^1H , ^{13}C , and ^{19}F NMR spectra, respectively), or Varian VNMRs 500 MHz (at 500 MHz, 125 MHz, and 470 MHz for ^1H , ^{13}C , and ^{19}F NMR spectra, respectively) spectrometers for solutions in CDCl_3 or $\text{DMSO}-d_6$ and TMS as the internal standard. Infrared (IR) spectra were recorded in the 4000–400 cm^{-1} region with a Jasco FT/IR-6200 spectrometer in KBr pallets. Mass spectra were measured with Synapt G2-S HDMS (*Waters Inc*) mass spectrometer equipped with an electrospray ion source and q-TOF type mass analyzer.

UV-vis absorption spectra were recorded using Perkin Elmer Lambda 35 spectrometer for *ca.* 10^{-5} M solutions of complexes. Emission spectra were recorded using Edinburgh Instruments' FLS980 Fluorescence Spectrometer ($\lambda_{\text{ex}} = 350$ nm) for *ca.* 10^{-5} M solutions and the solid-state samples of complexes. Thin solid films were prepared by using spin-coating technique utilizing SPS-Europe Spin150 Spin processor using 2.5 mg/ml solutions of the compounds in DCM on the pre-cleaned quartz substrates. Fluorescence quantum yields of the samples were estimated using the integrating sphere method. An integrating sphere (Edinburgh Instruments) coupled to the FLS980 spectrometer was calibrated with two standards: quinine sulfate in 0.1 M H_2SO_4 and rhodamine 6G in ethanol. Fluorescence decay curves of the solutions and of the solid films were recorded using a time-correlated single photon counting technique utilizing the PicoQuant PDL 820 picosecond pulsed diode laser as an excitation source ($\lambda_{\text{ex}} = 350$ nm). Electrochemical experiments were carried out using mAUTOLAB Type III apparatus, glassy carbon, silver wire and platinum coil as working, reference and auxiliary electrode, respectively.

Crystals of compounds **5** and **6a–f** were obtained by the slow evaporation of their solution in hexanes/DCM (1:1). The X-ray measurements were carried out at 100 K on SuperNova Agilent diffractometer using CuK α ($\lambda = 1.54184$ Å) radiation. Data reduction was done with *CrysAlisPro* (Agilent Technologies, *Version 1.171.35.21b*). The structures were solved by direct methods and refined using SHELXL Software Package.²¹ Crystallographic data of all investigated complexes have been deposited with the Cambridge Crystallographic Data Centre (CCDC). These data can be obtained, free of charge, from CCDC [e-mail: deposit@ccdc.cam.ac.uk or fax: +44(0)-1223-336033].

Synthesis

6-Bromobenzo[d]thiazol-2-amine (2b). A solution of bromine (155 μ L, 3.00 mmol) in glacial acetic acid (1 mL) was added dropwise to a solution of benzothiazole **2a** (451 mg, 3.00 mmol) in glacial acetic acid (10 mL). The reaction mixture was stirred at room temperature for 24 h and then was poured into cold water, and an aqueous solution of ammonium hydroxide (25%) was added to reach pH \sim 9. The precipitate was filtered, washed with water, dried, and recrystallized from ethanol to give product **2b** (626 mg, 2.73 mmol, 91%). Mp. 211.8–213.5 °C (lit.²² 213–214 °C), white powder. ¹H NMR (400 MHz, DMSO-*d*₆): δ = 7.87 (1H, d, J = 2.0 Hz), 7.58 (2H, s), 7.33 (1H, dd, J = 8.5 Hz, J = 2.0 Hz), 7.24 (1H, d, J = 8.5 Hz) ppm; ¹³C{¹H} NMR (100 MHz, DMSO-*d*₆): δ = 167.1, 152.0, 133.1, 128.2, 123.2, 119.1, 112.0 ppm. IR (KBr): 3270 (N-H), 3081 (N-H) cm⁻¹. HRMS (ESI-TOF) calcd for C₇H₆BrN₂S [M + H]⁺: 228.9430, found: 228.9427.

N-(6-Bromobenzo[d]thiazol-2-yl)-4-(dimethylamino)benzamide (4). To a solution of amine **2b** (459 mg, 2.00 mmol) in 1,4-dioxane (50 mL) were added 4-(dimethylamino)benzoyl chloride (**3**, 368 mg, 2.00 mmol), distilled trimethylamine (838 μ L, 6.00 mmol) and DMAP (12 mg, 0.10 mmol). The reaction mixture was refluxed for 24 h. After cooling, a saturated aqueous solution (50 mL) of NaHCO₃ were added and the mixture was extracted with DCM (3 \times 50 mL). The combined organic layers were dried over Na₂SO₄, filtered and concentrated. The product was purified by column chromatography (hexanes/DCM = 1:1 to 0:1, and next, DCM/MeOH = 99:1, v/v) to give amid **4** (491 mg, 1.30 mmol, 65%). Mp. 223.9–225.4 °C, yellowish powder. ¹H NMR (400 MHz, DMSO-*d*₆): δ = 12.49 (1H, br s), 8.22 (1H, s), 8.04 (2H, J = 8.6 Hz), 7.66 (1H, d, J = 8.6 Hz), 7.56 (1H, d, J = 8.6 Hz), 6.75 (2H, J = 8.6 Hz), 3.01 (6H, s) ppm; ¹³C{¹H} NMR (100 MHz, DMSO-*d*₆): δ = 165.2, 160.0, 153.2, 147.9, 133.9, 130.0 (2C), 128.9, 124.0, 121.7, 117.2,

115.1, 110.8 (2C), 39.6 (2C) ppm. IR (KBr): 3155 (N-H), 1662 (C-O) cm^{-1} . HRMS (ESI-TOF) calcd for $\text{C}_{16}\text{H}_{14}\text{N}_3\text{OSBrNa}$ $[\text{M} + \text{Na}]^+$: 397.9939, found: 397.9934.

4-(7-Bromo-1,1-difluoro-1H-1 λ^4 ,10 λ^4 -benzo[4,5]thiazolo[3,2-c][1,3,5,2]oxadiazaborinin-3-yl)-N,N-dimethylaniline (5). To a solution of amide **4** (452 mg, 1.20 mmol, 1 eq.) in dry DCM (40 mL) were added $\text{BF}_3 \cdot \text{Et}_2\text{O}$ (1.48 mL, 12.00 mmol, 10 eq.) and distilled DIPEA (4.19 mL, 24.00 mmol, 20 eq.) under an argon atmosphere. The reaction mixture was stirred for 24h at room temperature and then washed with water (3×30 mL). The organic phase was dried over anhydrous Na_2SO_4 , and filtered. The solvent was removed under reduced pressure and the crude product was purified by column chromatography (hexanes/dichloromethane from 1:1 to 0:1, v/v) to give complex **5** (376 mg, 0.89 mmol, 74%). Mp. 275.3–277.1 $^\circ\text{C}$, yellow powder. ^1H NMR (500 MHz, CDCl_3): δ = 8.25 (2H, d, J = 9.2 Hz), 7.86 (1H, d, J = 1.9 Hz), 7.82 (1H, d, J = 8.7 Hz), 7.64 (1H, dd, J = 8.7 Hz, J = 1.9 Hz), 6.69 (2H, d, J = 9.2 Hz), 3.13 (6H, s) ppm; $^{13}\text{C}\{^1\text{H}\}$ NMR (125 MHz, CDCl_3): δ = 173.7, 168.7, 154.8, 139.3, 133.2 (2C), 131.3, 128.2, 124.5, 119.0, 118.7, 116.7, 111.0 (2C), 40.1 (2C) ppm; ^{19}F NMR (470 MHz, CDCl_3): δ = – 137.55 (2F, m, BF_2) ppm. IR (KBr): 1610 (C=N) cm^{-1} . HRMS (ESI-TOF) calcd for $\text{C}_{16}\text{H}_{13}\text{BN}_3\text{OF}_2\text{SBr}$ $[\text{M}]^+$: 423.0024, found: 423.0027.

General procedure for the synthesis of complexes 6a–f. A mixture of bromo-compound **5** (51 mg, 0.12 mmol), aryl(thienyl)boronic acid (0.18 mmol), potassium carbonate (49 mg, 0.36 mmol), 1,4-dioxane (5 mL) and distilled water (2 mL) was degassed with a stream of argon passing through the solution for 15 min. Then, $\text{Pd}(\text{Ph}_3\text{P})_2\text{Cl}_2$ (8 mg, 0.01 mmol) was added and the reaction mixture was stirred under an argon atmosphere for 30 min at 80 $^\circ\text{C}$. After cooling, water (15 mL) was added and the mixture was extracted with DCM (3×20 mL). The collected organic phases were dried over Na_2SO_4 , filtered, and concentrated under reduced pressure. The residue was purified by flash chromatography on silica gel (hexanes/DCM = 2:1 to 1:4, v/v) to give product **6**.

4-(1,1-Difluoro-7-phenyl-1H-1 λ^4 ,10 λ^4 -benzo[4,5]thiazolo[3,2-c][1,3,5,2]oxadiazaborinin-3-yl)-N,N-dimethylaniline (6a): yellow powder (yield 45 mg, 89%). Mp: 277.1–279.5 $^\circ\text{C}$. ^1H NMR (500 MHz, CDCl_3): δ = 8.26 (2H, d, J = 9.1 Hz), 8.02 (1H, d, J = 8.6 Hz), 7.92 (1H, d, J = 1.6 Hz), 7.76 (1H, dd, J = 8.6 Hz, J = 1.6 Hz), 7.61 (2H, d, J = 7.8 Hz), 7.48 (2H, dd, J = 7.8 Hz, J = 7.4 Hz), 7.40 (1H, t, J = 7.4 Hz), 6.70 (2H, d, J = 9.1 Hz), 3.13 (6H, s, NMe_2) ppm; $^{13}\text{C}\{^1\text{H}\}$ NMR (125 MHz, CDCl_3): δ = 173.7, 168.4, 154.6, 139.8, 139.6, 139.3, 133.0 (2C), 129.0 (2C), 127.9, 127.4, 127.3, 127.3 (2C), 120.2, 118.0, 117.0, 111.0 (2C), 40.1 (2C) ppm; ^{19}F NMR (470 MHz, CDCl_3):

$\delta = -137.55$ (2F, m) ppm. IR (KBr): 1615 (C=N) cm^{-1} . HRMS (ESI-TOF) calcd for $\text{C}_{22}\text{H}_{18}\text{BN}_3\text{OF}_2\text{SNa}$ $[\text{M} + \text{Na}]^+$: 444.1129, found: 444.1122.

4-(1,1-Difluoro-7-(4-(trifluoromethyl)phenyl)-1H-1 λ^4 ,10 λ^4 -benzo[4,5]thiazolo[3,2-c][1,3,5,2]oxadiazaborinin-3-yl)-N,N-dimethylaniline (6b): yellow powder (yield 53 mg, 90%). Mp. 277.1–279.1 $^{\circ}\text{C}$. ^1H NMR (500 MHz, CDCl_3): $\delta = 8.27$ (2H, d, $J = 9.1$ Hz), 8.05 (1H, d, $J = 8.6$ Hz), 7.93 (1H, d, $J = 1.8$ Hz), 7.70–7.78 (5H, m), 6.71 (2H, d, $J = 9.1$ Hz), 3.14 (6H, s) ppm; ^{19}F NMR (470 MHz, CDCl_3): $\delta = -62.54$ (3F, s), -137.51 (2F, m) ppm. IR (KBr): 1609 (C=N) cm^{-1} . HRMS (ESI-TOF) calcd for $\text{C}_{23}\text{H}_{17}\text{BN}_3\text{OF}_5\text{SNa}$ $[\text{M} + \text{Na}]^+$: 512.1003, found: 512.1003.

4-(3-(4-(Dimethylamino)phenyl)-1,1-difluoro-1H-1 λ^4 ,10 λ^4 -benzo[4,5]thiazolo[3,2-c][1,3,5,2]oxadiazaborinin-7-yl)benzonitrile (6c): yellow powder (yield 45 mg, 84%). Mp. 290.8–292.5 $^{\circ}\text{C}$. ^1H NMR (500 MHz, CDCl_3): $\delta = 8.27$ (2H, d, $J = 9.2$ Hz), 8.05 (1H, d, $J = 8.5$ Hz), 7.93 (1H, d, $J = 2.0$ Hz), 7.77 (2H, d, $J = 8.5$ Hz), 7.75 (1H, dd, $J = 8.5$ Hz, $J = 2.0$ Hz), 7.72 (2H, d, $J = 8.5$ Hz), 6.71 (2H, d, $J = 9.2$ Hz), 3.14 (6H, s) ppm; $^{13}\text{C}\{^1\text{H}\}$ NMR (125 MHz, CDCl_3): $\delta = 174.1$, 168.6, 154.8, 144.2, 140.6, 137.0, 133.2 (2C), 132.8 (2C), 127.9 (2C), 127.6, 127.3, 120.5, 118.6, 118.3, 116.8, 111.6, 111.0 (2C), 40.1 (2C) ppm; ^{19}F NMR (470 MHz, CDCl_3): $\delta = -137.50$ (2F, m) ppm. IR (KBr): 2223 (CN), 1605 (C=N) cm^{-1} . HRMS (ESI-TOF) calcd for $\text{C}_{23}\text{H}_{17}\text{BN}_4\text{OF}_2\text{SNa}$ $[\text{M} + \text{Na}]^+$: 469.1082, found: 469.1079.

4-(1,1-Difluoro-7-(4-methoxyphenyl)-1H-1 λ^4 ,10 λ^4 -benzo[4,5]thiazolo[3,2-c][1,3,5,2]oxadiazaborinin-3-yl)-N,N-dimethylaniline (6d): yellow powder (yield 50 mg, 92%). Mp. 285.3–287.1 $^{\circ}\text{C}$. ^1H NMR (500 MHz, CDCl_3): $\delta = 8.26$ (2H, d, $J = 9.0$ Hz), 8.00 (1H, d, $J = 8.6$ Hz), 7.87 (1H, d, $J = 1.6$ Hz), 7.72 (1H, dd, $J = 8.6$ Hz, $J = 1.6$ Hz), 7.55 (2H, d, $J = 8.6$ Hz), 7.01 (2H, d, $J = 8.6$ Hz), 6.70 (2H, d, $J = 9.0$ Hz), 3.87 (3H, s), 3.13 (6H, s) ppm; $^{13}\text{C}\{^1\text{H}\}$ NMR (125 MHz, CDCl_3): $\delta = 173.4$, 168.3, 159.6, 154.6, 139.1, 139.0, 133.0 (2C), 132.3, 128.3 (2C), 127.4, 127.0, 119.6, 118.0, 117.1, 114.5 (2C), 111.0 (2C), 55.4, 40.1 (2C) ppm; ^{19}F NMR (470 MHz, CDCl_3): $\delta = -137.57$ (2F, m) ppm. IR (KBr): 1607 (C=N) cm^{-1} . HRMS (ESI-TOF) calcd for $\text{C}_{23}\text{H}_{20}\text{BN}_3\text{O}_2\text{F}_2\text{SNa}$ $[\text{M} + \text{Na}]^+$: 474.1235, found: 474.1227.

4,4'-(1,1-Difluoro-1H-1 λ^4 ,10 λ^4 -benzo[4,5]thiazolo[3,2-c][1,3,5,2]oxadiazaborinine-3,7-diyl)bis(N,N-dimethylaniline) (6e): orange powder (yield 54 mg, 97%). Mp. 312.5–314.7 $^{\circ}\text{C}$. ^1H NMR (400 MHz, CDCl_3): $\delta = 8.26$ (2H, d, $J = 9.1$ Hz), 7.97 (1H, d, $J = 8.7$ Hz), 7.86 (1H, d, $J = 1.6$ Hz), 7.72 (1H, dd, $J = 8.7$ Hz, $J = 1.6$ Hz), 7.52 (2H, d, $J = 8.9$ Hz), 6.82 (2H, d, $J = 8.9$ Hz), 6.70 (2H, d, $J = 9.1$ Hz), 3.12 (6H, s), 3.02 (6H, s) ppm; ^{19}F NMR (375 MHz, CDCl_3): $\delta = -137.62$

(2F, m) ppm. IR (KBr): 1610 (C=N) cm^{-1} . HRMS (ESI-TOF) calcd for $\text{C}_{24}\text{H}_{24}\text{BN}_4\text{OF}_2\text{S}$ $[\text{M} + \text{H}]^+$: 465.1732, found: 465.1733.

4-(1,1-Difluoro-7-(thiophen-2-yl)-1H-1 λ^4 ,10 λ^4 -benzo[4,5]thiazolo[3,2-

c][1,3,5,2]oxadiazaborinin-3-yl)-N,N-dimethylaniline (6f): yellow powder (yield 49 mg, 91%).

Mp. 297.2–299.0 $^{\circ}\text{C}$. ^1H NMR (500 MHz, CDCl_3): δ = 8.26 (2H, d, J = 9.2 Hz), 7.96 (1H, d, J = 8.5 Hz), 7.93 (1H, d, J = 1.8 Hz), 7.78 (1H, dd, J = 8.5 Hz, J = 1.8 Hz), 7.36 (1H, dd, J = 3.6 Hz, J = 1.0 Hz), 7.34 (1H, dd, J = 5.1 Hz, J = 1.0 Hz), 7.12 (1H, dd, J = 5.1 Hz, J = 3.6 Hz), 6.70 (2H, d, J = 9.2 Hz), 3.13 (6H, s) ppm; ^{19}F NMR (470 MHz, CDCl_3): δ = –137.55 (2F, m) ppm. IR (KBr): 1615 (C=N) cm^{-1} . HRMS (ESI-TOF) calcd for $\text{C}_{20}\text{H}_{16}\text{BN}_3\text{OF}_2\text{S}_2\text{Na}$ $[\text{M} + \text{Na}]^+$: 450.0694, found: 450.0685.

Keywords: boron complex • benzo[*d*]thiazole • thiazolo[3,2-*c*][1,3,5,2]oxadiazaborinine • Suzuki-Miyaura cross-coupling reaction • fluorescence

ASSOCIATED CONTENT

Supporting Information

The Supporting Information is available free of charge *via* the Internet at <http://pubs.acs.org> at DOI:

ORTEP diagrams for the X-ray structures and crystal data of complexes **5**, **6a–f**; Lippert–Mataga plots of **5**, **6a–f**; cyclic voltammograms of **5**, **6a–f**; optimized geometry for compounds **5**, **6a–f**; photophysical properties of complexes **6a–f** in the solid state; fluorescence decays of dyes **5**, **6a–f**; NMR and IR spectra of all synthesized compounds(PDF)

Crystal data of **5** (CIF)

Crystal data of **6a** (CIF)

Crystal data of **6b** (CIF)

Crystal data of **6c** (CIF)

Crystal data of **6d** (CIF)

Crystal data of **6e** (CIF)

Crystal data of **6f** (CIF)

AUTHOR INFORMATION

Corresponding Author

*E-mail: potopnyk@gmail.com

ORCID

Mykhaylo A. Potopnyk: 0000-0002-4543-2785

Dmytro Volyniuk: 0000-0003-3526-2679

Roman Luboradzki: 0000-0001-8910-230X

Magdalena Ceborska: 0000-0001-5555-771X

Iryna Hladka: 0000-0002-6864-4254

Yan Danyliv: 0000-0001-9645-0337

Juozas V. Grazulevicius: 0000-0002-4408-9727

ACKNOWLEDGMENTS

We gratefully acknowledge the financial support from Institute of Organic Chemistry of the Polish Academy of Sciences, European Social Fund (the activity ‘Improvement of researchers’ qualification by implementing world-class R&D projects’ of Measure No. 09.3.3-LMT-K-712), and Institute of Physical Chemistry of the Polish Academy of Sciences.

REFERENCES

(1) (a) Yang, Z.; Mao, Z.; Xie, Z.; Zhang, Y.; Liu, S.; Zhao, J.; Xu, J.; Chi, Z.; Aldred, M. P. Recent advances in organic thermally activated delayed fluorescence materials. *Chem. Soc. Rev.* **2017**, *46*, 915–1016; (b) Costa, R. D.; Ortí, E.; Bolink, H. J.; Monti, F.; Accorsi, G.; Armaroli, N. Luminescent Ionic Transition-Metal Complexes for Light-Emitting Electrochemical Cells. *Angew. Chem. Int. Ed.* **2012**, *51*, 8178–8211; (c) Frath, D.; Massue, J.; Ulrich, G.; Ziessel, R. Luminescent Materials: Locking π -Conjugated and Heterocyclic Ligands with Boron(III). *Angew. Chem., Int. Ed.* **2014**, *53*, 2290–2310.

(2) (a) Dsouza, R. N.; Pischel, U.; Nau, W. M. Fluorescent Dyes and Their Supramolecular Host/Guest Complexes with Macrocycles in Aqueous Solution. *Chem. Rev.* **2011**, *111*, 7941–7980; (b) Wang, H.; Ji, X.; Li, Z.; Huang, F. Fluorescent Supramolecular Polymeric Materials. *Adv. Mater.* **2017**, *29*, 1606117; (c) Mako, T. L.; Racicot, J. M.; Levine, M. Supramolecular Luminescent Sensors. *Chem. Rev.* **2019**, *119*, 322–477.

(3) (a) Hou, J.-T.; Ren, W. X.; Li, K.; Seo, J.; Sharma, A.; Yu, X.-Q.; Kim, J. S. Fluorescent Bioimaging of pH: from Design to Applications. *Chem. Soc. Rev.* **2017**, *46*, 2076–2090; (b) Zhang, K. Y.; Yu, Q.; Wei, H.; Liu, S.; Zhao, Q.; Huang, W.; Long-Lived Emissive Probes for Time-Resolved Photoluminescence Bioimaging and Biosensing. *Chem. Rev.* **2018**, *118*, 1770–1839.

(4) (a) Loudet, A.; Burgess, K. BODIPY Dyes and Their Derivatives: Syntheses and Spectroscopic Properties. *Chem. Rev.* **2007**, *107*, 4891–4932; (b) Bessette, A.; Hanan, G. S. Design, Synthesis and Photophysical Studies of Dipyrrromethene-based Materials: Insights into Their Applications in Organic Photovoltaic Devices. *Chem. Soc. Rev.* **2014**, *43*, 3342–3405; (c) Kowada, T.; Maeda, H.; Kikuchi, K. BODIPY-based Probes for the Fluorescence Imaging of Biomolecules in Living Cells. *Chem. Soc. Rev.* **2015**, *44*, 4953–4972.

(5) (a) Grabarz, A. M.; Laurent, A. D.; Jędrzejewska, B.; Zakrzewska, A.; Jacquemin, D.; Ośmiałowski, B. The Influence of the π -Conjugated Spacer on Photophysical Properties of Difluoroboranyls Derived from Amides Carrying a Donor Group. *J. Org. Chem.* **2016**, *81*, 2280–

2292; (b) Bonacorso, H. G.; Calheiro, T. P.; Iglesias, B. A.; Acunha, T. V.; Franceschini, S. Z.; Ketzer, A.; Meyer, A. R.; Rodrigues, L. V.; Nogara, P. A.; Rocha, J. B. T.; Zanatta, N.; Martins, M. A. P. 1,1-Difluoro-3-aryl(heteroaryl)-1*H*-pyrido[1,2-*c*][1,3,5,2]oxadiazaborinin-9-ium-1-uides: Synthesis; Structure; and Photophysical, Electrochemical, and BSA-Binding Studies. *New J. Chem.* **2018**, 42, 1913–1920; (c) Yamaji, M.; Kato, S.; Tomonari, K.; Mamiya, M.; Goto, K.; Okamoto, H.; Nakamura, Y.; Tani, F. Blue Fluorescence from BF₂ Complexes of *N,O*-Benzamide Ligands: Synthesis, Structure, and Photophysical Properties. *Inorg. Chem.* **2017**, 56, 12514–12519.

(6) (a) Hachiya, S.; Inagaki, T.; Hashizume, D.; Maki, S.; Niwa, H.; Hirano, T. Synthesis and Fluorescence Properties of Difluoro[amidopyrazinato-*O,N*]boron Derivatives: A New Boron-Containing Fluorophore. *Tetrahedron Lett.* **2010**, 51, 1613–1615; (b) Hachiya, S.; Hashizume, D.; Ikeda, H.; Yamaji, M.; Maki, S.; Niwa, H.; Hirano, T. Spectroscopic properties of BF₂ complexes of *N*-(5-phenyl-2-pyrazinyl) pivalamides exhibiting fluorescence in solution and solid state. *J. Photochem. Photobiol. A: Chem.* **2016**, 331, 206–214.

(7) (a) Du, M.-L.; Hu, C.-Y.; Wang, L.-F.; Li, C.; Han, Y.-Y.; Gan, X.; Chen, Y.; Mu, W.-H.; Huang, M. L.; Fu, W.-F. New Members of Fluorescent 1,8-Naphthyridine-Based BF₂ Compounds: Selective Binding of BF₂ with Terminal Bidentate N^NN^O and N^C^O Groups and Tunable Spectroscopy Properties. *Dalton Trans.* **2014**, 43, 13924–13931; (b) Wu, Y.-Y.; Chen, Y.; Gou, G.-Z.; Mu, W.-H.; Lv, X.-J.; Du, M.-L.; Fu, W.-F. Large Stokes Shift Induced by Intramolecular Charge Transfer in *N,O*-Chelated Naphthyridine–BF₂ Complexes. *Org. Lett.* **2012**, 14, 5226–5229; (c) Wu, Y.-Y.; Chen, Y.; Mu, W.-H.; Lv, X.-J.; Fu, W.-F. Naphthyridine–BF₂ Complexes with an Amide-Containing Di-2-picolylamine Receptor: Synthesis, Structures and Photo-Induced Electron Transfer. *J. Photochem. Photobiol. A: Chem.* **2013**, 272, 73–79; (d) Wu, G. F.; Xu, Q. L.; Guo, L. E.; Zang, T. N.; Tan, R.; Tao, S. T.; Ji, J. F.; Hao, R. T.; Zhang, J. F.; Zhou, Y. 1,8-Naphthyridine-Based Boron Complexes: Visible Colorimetric Probes for Highly Selective Sensing of Phosphoric Ion. *Tetrahedron Lett.* **2015**, 56, 5034–5038; (e) Bonacorso, H. G.; Calheiro, T. P.; Iglesias, B. A.; Berni, I. R. C.; da Silva Júnior, E. N.; Rocha, J. B. T.; Zanatta, N.; Martins, M. A. P. Synthesis, ¹¹B- and ¹⁹F NMR Spectroscopy, and Optical and Electrochemical Properties of Novel 9-Aryl-3-(aryl/heteroaryl)-1,1-difluoro-7-(trifluoromethyl)-1*H*-[1,3,5,2]oxadiazaborinino[3,4-*a*][1,8]naphthyridin-11-ium-1-uide Complexes. *Tetrahedron Lett.* **2016**, 57, 5017–5021.

(8) Zhang, K.; Zheng, H.; Hua, C.; Xin, M.; Gao, J.; Li, Y. Novel Fluorescent *N,O*-Chelated Fluorine-Boron Benzamide Complexes Containing Thiadiazoles: Synthesis and Fluorescence Characteristics. *Tetrahedron* **2018**, 74, 4161–4167.

(9) (a) Potopnyk, M. A.; Lytvyn, R.; Danyliv, Y.; Ceborska, M.; Bezvikonnyi, O.; Volyniuk, D.; Gražulevičius, J. V. *N,O* π -Conjugated 4-Substituted 1,3-Thiazole BF₂ Complexes: Synthesis and Photophysical Properties. *J. Org. Chem.* **2018**, 83, 1095–1105; (b) Potopnyk, M. A.; Lytvyn, R.; Danyliv, Y.; Ceborska, M.; Bezvikonnyi, O.; Volyniuk, D.; Gražulevičius, J. V. Correction to *N,O* π -Conjugated 4-Substituted 1,3-Thiazole BF₂ Complexes: Synthesis and Photophysical Properties. *J. Org. Chem.* **2018**, 83, 5876.

(10) Potopnyk, M. A.; Volyniuk, D.; Ceborska, M.; Cmoch, P.; Hladka, I.; Danyliv, Y.; Gražulevičius, J. V. Benzo[4,5]thiazolo[3,2-*c*][1,3,5,2]oxadiazaborinines: Synthesis, Structural, and Photophysical Properties. *J. Org. Chem.* **2018**, 83, 12129–12142.

(11) (a) Segawa, Y.; Maekawa, T.; Itami, K. Synthesis of Extended π -Systems through C–H Activation *Angew. Chem. Int. Ed.* **2015**, 54, 66–81; (b) Pouliot, J.-R.; Grenier, F.; Blaskovits, J.

T.; Beaupré, S.; Leclerc, M. Direct (Hetero)arylation Polymerization: Simplicity for Conjugated Polymer Synthesis. *Chem. Rev.* **2016**, *116*, 14225–14274.

(12) (a) Shi, W.; Liu, C.; Lei, A. Transition-Metal Catalyzed Oxidative Cross-Coupling Reactions to form C–C Bonds Involving Organometallic Reagents as Nucleophiles. *Chem. Soc. Rev.* **2011**, *40*, 2761–2776; (b) So, C. M.; Kwong, F. Y. Palladium-Catalyzed Cross-Coupling Reactions of Aryl Mesylates. *Chem. Soc. Rev.* **2011**, *40*, 4963–4972.

(13) (a) Leen, V.; Miscoria, D.; Yin, S.; Filarowski, A.; Ngongo, J. M.; Van der Auweraer, M.; Boens, N.; Dehaen, W. 1,7-Disubstituted Boron Dipyrromethene (BODIPY) Dyes: Synthesis and Spectroscopic Properties. *J. Org. Chem.* **2011**, *76*, 8168–8176; (b) Leen, V.; Yuan, P.; Wang, L.; Boens, N.; Dehaen, W. Synthesis of Meso-Halogenated BODIPYs and Access to Meso-Substituted Analogues. *Org. Lett.* **2012**, *14*, 6150–6153; (c) Feng, Z.; Jiao, L.; Feng, Y.; Yu, C.; Chen, N.; Wei, Y.; Mu, X.; Hao, E. Regioselective and Stepwise Syntheses of Functionalized BODIPY Dyes through Palladium-Catalyzed Cross-Coupling Reactions and Direct C–H Arylations. *J. Org. Chem.* **2016**, *81*, 6281–6291; (d) Chong, H.; Fron, E.; Liu, Z.; Boodts, S.; Thomas, J.; Harvey, J. N.; Hofkens, J.; Dehaen, W.; Van der Auweraer, M.; Smet, M. Acid-Sensitive BODIPY Dyes: Synthesis through Pd-Catalyzed Direct C(sp³)–H Arylation and Photophysics. *Chem. Eur. J.* **2017**, *23*, 4687–4699.

(14) (a) Meares, A.; Satraitis, A.; Akhigbe, J.; Santhanam, N.; Swaminathan, S.; Ehudin, M.; Ptaszek, M. Amphiphilic BODIPY-Hydroporphyrin Energy Transfer Arrays with Broadly Tunable Absorption and Deep Red/Near-Infrared Emission in Aqueous Micelles. *J. Org. Chem.* **2017**, *82*, 6054–6070; (b) Arroyo-Córdoba, I. J.; Sola-Llano, R.; Epelde-Elezcano, N.; López Arbeloa, I.; Martínez-Martínez, V.; Peña-Cabrera, E. Fully Functionalizable β,β' -BODIPY Dimer: Synthesis, Structure, and Photophysical Signatures. *J. Org. Chem.* **2018**, *83*, 10186–10196; (c) Taguchi, D.; Nakamura, T.; Horiuchi, H.; Saikawa, M.; Nabeshima, T. Synthesis and Unique Optical Properties of Selenophenyl BODIPYs and Their Linear Oligomers. *J. Org. Chem.* **2018**, *83*, 5331–5337; (d) Xuan, S.; Zhao, N.; Ke, X.; Zhou, Z.; Fronczek, F. R.; Kadish, K. M.; Smith, K. M.; Vicente, M. G. H. Synthesis and Spectroscopic Investigation of a Series of Push–Pull Boron Dipyrromethenes (BODIPYs). *J. Org. Chem.* **2017**, *82*, 2545–2557.

(15) Chapran, M.; Angioni, E.; Findlay, N. J.; Breig, B.; Cherpak, V.; Stakhira, P.; Tuttle, T.; Volyniuk, D.; Grazulevicius, J. V.; Nastishin, Y. A.; Lavrentovich, O. D.; Skabara, P. J. An Ambipolar BODIPY Derivative for a White Exciplex OLED and Cholesteric Liquid Crystal Laser toward Multifunctional Devices. *ACS Appl. Mater. Interfaces* **2017**, *9*, 4750–4757.

(16) (a) Verbelen, B.; Leen, V.; Wang, L.; Boens, N.; Dehaen, W. Direct Palladium-Catalysed C–H Arylation of BODIPY Dyes at the 3- and 3,5-Positions. *Chem. Commun.* **2012**, *48*, 9129–9131; (b) Verbelen, B.; Boodts, S.; Hofkens, J.; Boens, N.; Dehaen, W. Radical C–H Arylation of the BODIPY Core with Aryldiazonium Salts: Synthesis of Highly Fluorescent Red-Shifted Dyes. *Angew. Chem. Int. Ed.* **2015**, *54*, 4612–4616; (c) Chong, H.; Lin, H.-A.; Shen, M.-Y.; Liu, C.-Y.; Zhao, H.; Yu, H. Step-Economical Syntheses of Functional BODIPY-EDOT π -Conjugated Materials through Direct C–H Arylation. *Org. Lett.* **2015**, *17*, 3198–3201.

(17) Hand, E. S.; Baker, D. C. Syntheses of 2-Chloro- and 2-Amino-5-fluoropyridines and Isolation of a Novel Difluoroboryl Imidate. *Synthesis* **1989**, 905–908.

(18) Savoldelli, A.; Meng, Q.; Paolesse, R.; Fronczek, F. R.; Smith, K. M.; Vicente, M. G. H. Tetrafluorobenzo-Fused BODIPY: A Platform for Regioselective Synthesis of BODIPY Dye Derivatives. *J. Org. Chem.* **2018**, *83*, 6498–6507.

(20) Frisch, M. J.; Trucks, G. W.; Schlegel, H. B.; Scuseria, G. E.; Robb, M. A.; Cheeseman, J. R.; Scalmani, G.; Barone, V.; Mennucci, B.; Petersson, G. A.; Nakatsuji, H.; Caricato, M.; Li, X.; Hratchian, H. P.; Izmaylov, A. F.; Bloino, J.; Zheng, G.; Sonnenberg, J. L.; Hada, M.; Ehara, M.; Toyota, K.; Fukuda, R.; Hasegawa, J.; Ishida, M.; Nakajima, T.; Honda, Y.; Kitao, O.; Nakai, H.; Vreven, T.; Montgomery, J. A., Jr.; Peralta, J. E.; Ogliaro, F.; Bearpark, M.; Heyd, J. J.; Brothers, E.; Kudin, K. N.; Staroverov, V. N.; Keith, T.; Kobayashi, R.; Normand, J.; Raghavachari, K.; Rendell, A.; Burant, J. C.; Iyengar, S. S.; Tomasi, J.; Cossi, M.; Rega, N.; Millam, J. M.; Klene, M.; Knox, J. E.; Cross, J. B.; Bakken, V.; Adamo, C.; Jaramillo, J.; Gomperts, R.; Stratmann, R. E.; Yazyev, O.; Austin, A. J.; Cammi, R.; Pomelli, C.; Ochterski, J. W.; Martin, R. L.; Morokuma, K.; Zakrzewski, V. G.; Voth, G. A.; Salvador, P.; Dannenberg, J. J.; Dapprich, S.; Daniels, A. D.; Farkas, O.; Foresman, J. B.; Ortiz, J. V.; Cioslowski, J.; Fox, D. J. *Gaussian 09*, revision D.01; Gaussian, Inc.: Wallingford, CT, USA, 2013.

(21) Sheldrick, G. M. A Short History of SHELX. *Acta Cryst.* **2008**, *A64*, 112–122.

(22) Hrobáriková, V.; Hrobárik, P.; Gajdoš, P.; Fítilis, I.; Fakis, M.; Persephonis, P.; Zahradník, P. Benzothiazole-Based Fluorophores of Donor- π -Acceptor- π -Donor Type Displaying High Two-Photon Absorption. *J. Org. Chem.* **2010**, *75*, 3053–3068.